The EMBO Journal Vol.16 No.8 pp.1858–1864, 1997

Unrestrained nociceptive response and disregulation of hearing ability in mice lacking the nociceptin/orphaninFQ receptor

Miyuki Nishi[1], Takeshi Houtani[2], Yukihiro Noda[3], Takayoshi Mamiya[3], Kazuo Sato[4], Tadashi Doi[4], Junko Kuno[5], Hiroshi Takeshima[1,6], Toshihide Nukada[1], Toshitaka Nabeshima[3], Toshio Yamashita[4], Tetsuo Noda[5] and Tetsuo Sugimoto[2]

[1]Department of Neurochemistry, Tokyo Institute of Psychiatry, Kamikitazawa, Setagaya-ku, Tokyo 156, [2]Department of Anatomy and [4]Department of Otolaryngology, Kansai Medical University, Moriguchi, Osaka 570, [3]Department of Neuropsychopharmacology and Hospital Pharmacy, Nagoya University School of Medicine, Showa-ku, Nagoya 466 and [5]Department of Cell Biology, Cancer Institute, Kami-Ikebukuro, Toshima-ku, Tokyo 170, Japan

[6]Present address: Department of Pharmacology, Faculty of Medicine, University of Tokyo, 7-3-1 Hongo, Bunkyo-ku, Tokyo 113, Japan

[6]Corresponding author

In the G-protein-coupled receptor superfamily, the opioid receptor subfamily is constituted of the three distinct opioid receptors (namely δ-, μ- and κ-subtypes) and the receptor for nociceptin (also designated orphaninFQ). The members of the opioid receptor subfamily were known to mediate a variety of cellular inhibitory effects. The three opioid receptors are known to play central roles in mediating analgesia and many other physiological activities; however, the nociceptin receptor was identified recently and less is known about its physiological roles. Here we report the generation and characterization of mice lacking the nociceptin receptor. The knockout mice showed no significant differences in nociceptive threshold and locomotor activity compared with control mice, but they lost nociceptin-induced behavioral responses. These results indicate that the nociceptin system is not essential for regulation of nociception or locomotor activity. On the other hand, we found insufficient recovery of hearing ability from the adaptation to sound exposure in the mutant mice. Thus, the nociceptin system appears to participate in the regulation of the auditory system.

Keywords: auditory brainstem response/nociceptin/nociception/opioid receptor/orphaninFQ

Introduction

Multiple binding sites for opioid ligands have been identified based on pharmacological studies, and the opioid receptors have been shown to mediate a variety of cellular inhibitory effects, including inhibition of adenylate cyclase, activation of potassium channels and inhibition of calcium channels (Loh and Smith, 1990). Previous DNA cloning studies have shown that in the G-protein-linked receptor superfamily (Hille, 1992) the opioid receptor subfamily is constituted of three opioid receptors (designated as δ-, μ- and κ-subtypes) and an opioid receptor homolog, termed ORL1, ROR-C or LC132 (Bunzow *et al.*, 1994; Fukuda *et al.*, 1994; Mollereau *et al.*, 1994; Knapp *et al.*, 1995). Despite a high degree of amino acid sequence similarity between the members of the opioid receptor subfamily, the opioid receptor homologs expressed from the cDNAs did not show high affinities for opioid ligands. Recently, nociceptin, also designated orphaninFQ, has been identified as a novel peptide agonist for the opioid receptor homolog from the brain (Meunier *et al.*, 1995; Reinscheid *et al.*, 1995). Nociceptin is derived from a larger precursor which shows sequence similarity to the opioid peptide precursors, particularly pre-prodynorphin (Houtani *et al.*, 1996; Mollereau *et al.*, 1996; Nothacker *et al.*, 1996). Thus, the nociceptin system is closely related to the opioid peptide system structurally, evolutionarily and functionally.

So far, several groups have reported the biological functions of the nociceptin system. In contrast to the opioid peptides with analgesic effects, nociceptin induced hyperalgesia or allodynia, when administered intracerebroventricularly (i.c.v.) or intrathecally, respectively (Meunier *et al.*, 1995; Okuda-Ashitaka *et al.*, 1996). Nociceptin caused a decrease in locomotor activity (Reinscheid *et al.*, 1995). Inhibition of expression of the nociceptin receptor reduced immunoglobulin production, and a mitogen induced expression of nociceptin receptor mRNA in lymphocytes (Halford *et al.*, 1995; Wick *et al.*, 1995). Expression of nociceptin precursor mRNA was regulated by intracellular cAMP levels in NS20Y neuroblastoma cells (Saito *et al.*, 1996). The reported results suggested important roles for the nociceptin system in modulation of the nociceptive threshold, locomotor activity, immunological responses and neuronal development. However, specific antagonists for the nociceptin receptor are not available, and the physiological roles of the nociceptin system have not been elucidated yet at the whole-animal level. One approach to this issue would be to produce mutant mice lacking the nociceptin receptor by means of the gene targeting technique and to analyze the physiological phenotypes of the mutants. We report here the generation of mice with a targeted mutation in the nociceptin receptor gene. Although the mutant mice showed no abnormalities in nociception, locomotion and the immune system, we found abnormal hearing ability in the mutants. The results clearly demonstrated an essential role for the nociceptin system in regulation of the auditory system.

Results and discussion

Generation of mutant mice lacking the nociceptin receptor

As shown in Figure 1A, genomic DNA fragments from the mouse nociceptin receptor gene (Nishi *et al.*, 1994)

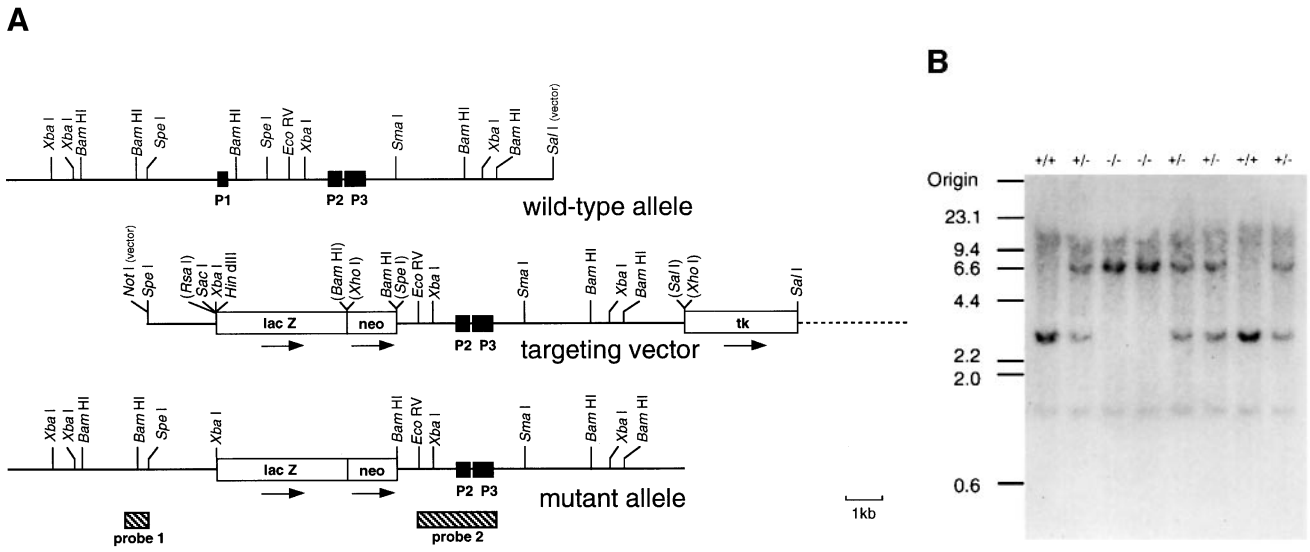

Fig. 1. (**A**) Targeting of the nociceptin receptor gene by homologous recombination. Restriction enzyme maps of the wild-type allele, targeting vector and expected mutant locus are illustrated. The protein-coding sequences (P1–P3) are indicated by filled boxes. The β-galactosidase gene (*lacZ*), neomycin-resistance gene (*neo*) and virus thymidine kinase gene (*tk*) are shown by open boxes; the transcriptional directions are indicated by arrows. In the targeting vector, restriction enzyme sites used for construction and linearization are also shown; enzyme sites in parentheses are deleted by the construction. For detection of the targeted mutation, a synthetic linker was introduced between the 5′ genomic and *lacZ* fragments in the vector. (**B**) Southern blot of tail DNAs from littermates obtained by crossing between the heterozygous mutants. *Bam*HI-digested DNA was analyzed using the probe 1 shown in (A). The 2.7 and 7.1 kb fragments are expected from the wild-type and mutant allele, respectively, and the 1.6 kb fragment is expected from both alleles. The size markers are indicated in kbp.

were used to construct a targeting vector, in which the first protein-coding sequence (P1) is replaced with a *lacZ–neo* cassette and the sequence of the *lacZ* gene encoding bacterial β-galactosidase is linked to the 5′-non-coding sequence. In the expected mutant allele, it is thus possible to express the *lacZ* gene under the control of the transcription machinery of the nociceptin receptor gene. The gene targeting and generation of mutant mice were performed essentially as described previously (Takeshima *et al.*, 1994); in the experimental procedures, we used J1 embryonic stem (ES) cells derived from a 129 strain mouse (Li *et al.*, 1992) and C57BL/6J mice to cross with chimeric males. Two lines of mice carrying the mutant allele designated as *morc*^{m1} were established using independent ES clones positive in Southern blot analysis (Figure 1B).

RNA blot hybridization analysis failed to detect mRNA for the nociceptin receptor in the brains of the homozygous mice (Figure 2A); therefore, the *morc*^{m1} mutation seems to be a null mutation in the gene. On the other hand, the expression levels of nociceptin precursor mRNA are comparable in the brains of mutant and control mice (Figure 2B). The homozygous mice obtained were healthy and fertile, and we could not find any anatomical abnormalities in the mutants. Two lines of the nociceptin receptor-deficient mice yielded essentially the same results in the experiments described below.

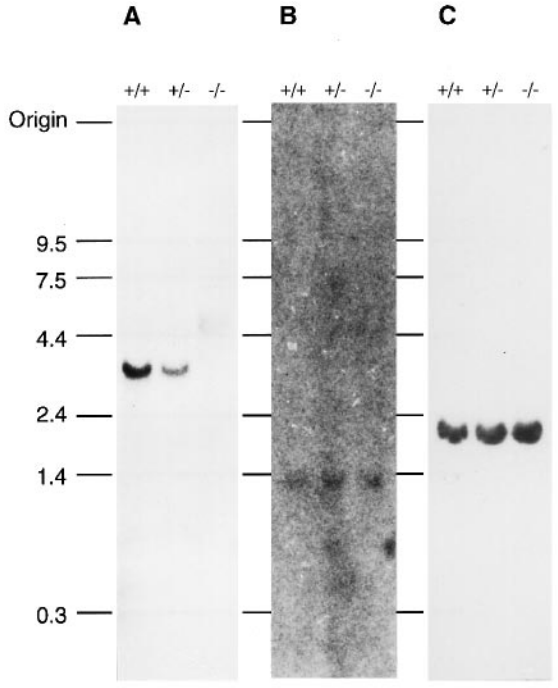

Fig. 2. Autoradiograms of blot hybridization analysis of RNA from brains of adult mice, using the genomic DNA probe (probe 2 indicated in Figure 1A) for nociceptin receptor mRNA in (**A**), the cDNA probe (Houtani *et al.*, 1996) for nociceptin precursor mRNA in (**B**) and the cDNA probe (Clontech Laboratories, Inc.) for β-actin mRNA in (**C**). The data were derived from a blotting sheet re-used successively. The size markers are indicated in kb.

Nociception in mice lacking the nociceptin receptor

Because hyperalgesia and allodynia induced by nociceptin have been reported (Meunier *et al.*, 1995; Okuda-Ashitaka *et al.*, 1996), we conducted the heat tail-flick test to compare nociceptive thresholds in the nociceptin receptor-deficient and control mice (Figure 3A and B). If the nociceptin system functioned as a major regulator in the nociceptive system, the loss of the nociceptin receptor might result in anti-nociceptive effects in the mutant mice. In accordance with the reported data, nociceptin induced hyperalgesia when administered i.c.v. to wild-type mice. In contrast, we could not find a significant difference in

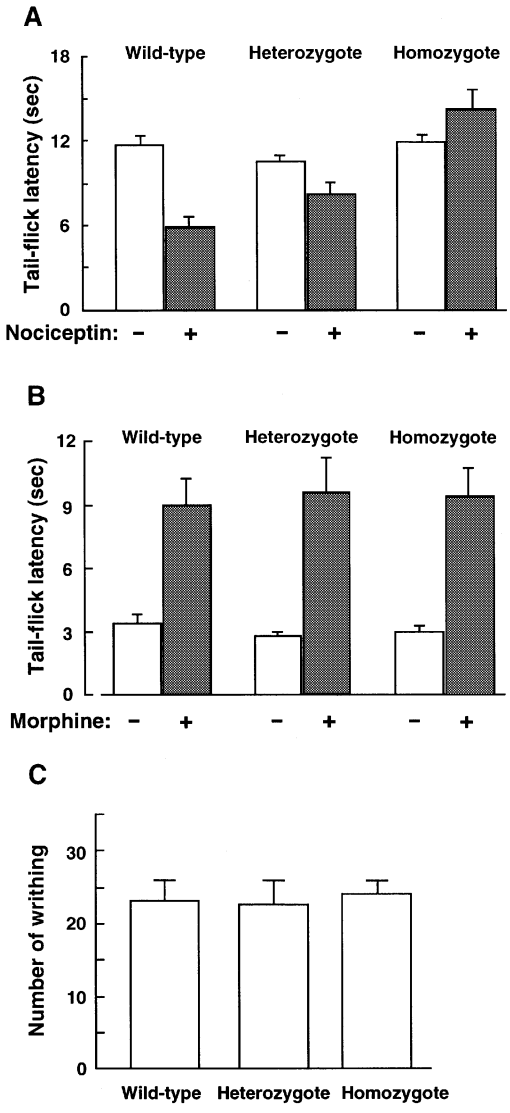

Fig. 3. (**A**) Nociceptive threshold and hyperalgesic effects of nociceptin in nociceptin receptor-deficient mice. The tail-flick latencies in mice injected with or without nociceptin (10 nmol, i.c.v.) are shown as the mean ± SEM (n = 4–8 in each group). Administration of a lower dose of nociceptin (1 nmol, i.c.v.) did not affect the tail-flick latency in each group (data not shown). (**B**) Anti-nociceptive effect of morphine in the nociceptin receptor-deficient mice. The tail-flick latencies in mice injected with or without morphine (10 mg/kg, s.c.) are shown as the mean ± SEM (n = 7–9 in each group). The heat stimuli differ in light intensity between experiments in (A) and (B). (**C**) Nociceptive threshold examined by the acetic acid-induced writhing behavior in nociceptin receptor-deficient mice. The numbers of writhing are shown as the mean ± SEM (n = 20–22 in each group).

the latency of the tail-flick response to heat between the untreated homozygous mutants and those treated with nociceptin. However, no measurable difference in nociceptive thresholds was observed between the untreated mutant and control mice under different conditions of heat intensity (Figure 3A and B). Moreover, we also examined nociceptive thresholds in the test using acetic acid-induced writhing behavior, a test that allows a more sensitive detection of the thresholds than the tail-flick test (Figure 3C). Again the mutant mice showed nociceptive thresholds comparable with that of control mice.

The results clearly show that nociceptin-induced hyperalgesia is mediated by the product derived from the nociceptin receptor gene, and also indicate that regulation by the nociceptin system is not essential for the determination of the nociceptive threshold *in vivo*. However, our data cannot eliminate the possibility that neuromodulation systems other than the nociceptin system, for example opioid peptide systems, may compensate for abnormalities in the mutant mice. On the other hand, the loss of the nociceptin system does not affect the morphine-induced anti-nociceptive response (Figure 3B). Recently, it was reported that mutant mice lacking the μ-opioid receptor lost morphine-induced anti-nociceptive effects but showed an apparently normal nociceptive threshold (Matthes *et al.*, 1996). Together these observations may suggest that the nociceptive threshold is regulated by highly compensating mechanisms in the central nervous system.

Locomotion in mice lacking the nociceptin receptor

The spontaneous locomotor activity of the mutant mice was then examined because reduction of locomotor activity by nociceptin administration was observed (Reinscheid *et al.*, 1995). Assuming that the nociceptin system was a dominant modulation system in locomotor activity, hyperactivities might be expected in the mutant mice. However, the results showed a slightly reduced locomotor activity of the homozygous mutants as compared with that of control mice (Figure 4). We also examined the effects of nociceptin administration on locomotor activity. Nociceptin-induced hypoactivity was observed in wild-type mice as reported previously, but we could not detect any obvious effect of nociceptin in the homozygous mutants (Figure 4). These results show that disruption of the nociceptin receptor gene results in the loss of nociceptin-induced hypolocomotion.

The results of nociceptin-induced hypolocomotion in wild-type mice and the tendency to hypolocomotion in the homozygous mutants seem to be mutually exclusive. However, these results could be compatible because locomotor activity is controlled by highly complex neural circuits interconnecting the sensory and motor systems. Alternatively, it may be that the reduced locomotor activity in the homozygous mutants is due to the genetic background rather than the loss of the nociceptin receptor. In our targeting procedures, the genetic background of the 129 strain rather than the C57BL mouse would have the predominating influence in the homozygous mutant. Strain 129 mice exhibit a significant locomotor hypoactivity in comparison with C57BL mice, and the majority of knockout mice with the mixed 129–C57BL genotype exhibit hypoactivity (Gerlai, 1996). Nevertheless, the absence of any obvious abnormality in locomotor activity of the mutant mice suggests that the nociceptin system is not a major determinant in the regulation of locomotion in the central nervous system.

The immune system in mice lacking the nociceptin receptor

It was reported that antisense oligonucleotides for the nociceptin receptor inhibit immunoglobulin production in B-lymphocytes and that mitogen stimulation resulted in a remarkable induction of the level of nociceptin receptor

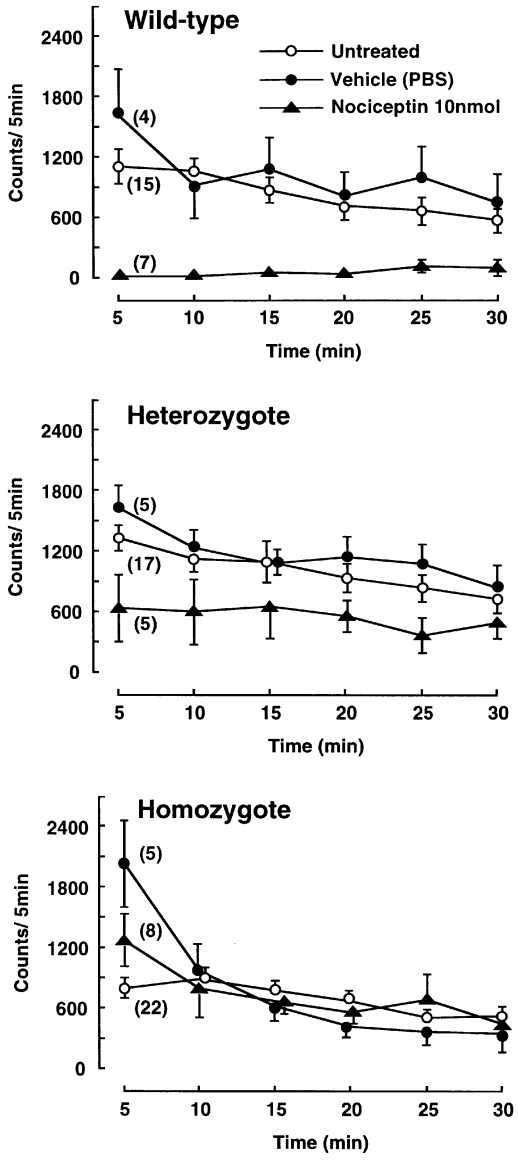

Fig. 4. Locomotor activity in nociceptin receptor-deficient mice. Locomotor count was recorded over 30 min; results were analyzed as a block of 5 min and are shown as the mean ± SEM. The effects of the targeted mutation were tested using untreated mice (○). In the comparisons of total locomotor counts during 30 min, statistical analysis (Neuman–Keuls test) revealed a difference between untreated homozygote and wild-type groups ($P < 0.05$) and no significant difference between untreated heterozygote and wild-type groups. To examine the effects of nociceptin, mice injected with phosphate-buffered saline (●) or nociceptin (10 nmol, i.c.v.) (▲) were tested. Significant nociceptin-induced hypoactivity was observed in wild-type mice ($P < 0.01$) but not in homozygous mutants. No detectable effect was observed in mice treated with a lower dose of nociceptin (1 nmol) in each genotype group (data not shown).

mRNA in peripheral blood lymphocytes (Halfold *et al.*, 1995; Wick *et al.*, 1995). These observations may suggest important immunological roles for the nociceptin system. However, we detected no abnormalities in the immunoglobulin content of peripheral blood from nociceptin receptor-deficient mice (data not shown). Moreover, in flow cytometric analysis using antibodies to specific cell surface markers, we identified no abnormal populations of T- and B-lymphocytes in the blood and bone marrow (data not shown). These results suggest that the nociceptin system is not essential for lymphocyte proliferation and immunoglobulin production.

Regional distribution of the nociceptin receptor and nociceptin precursor

As expected from the targeting construct, neurons expressing the nociceptin receptor can be detected by β-galactosidase activity in the mutant mice. Indeed, the regions positive in X-gal staining in brain and spinal cord from mutants (Figure 5A–G) almost correspond with the areas positive in previous *in situ* experiments with antisense probes for the nociceptin receptor mRNA (Fukuda *et al.*, 1994; Mollereau *et al.*, 1994). Furthermore, the brain and spinal cord areas with predominant expression of the nociceptin precursor message (Figure 5H–K) appeared identical to the sites that exhibit significant levels of β-galactosidase activity (Figure 5E–G). These results, together with our previous observations (Houtani *et al.*, 1996), indicate that the nociceptin receptor in these sites may be located on, or afforded many synapses by, nociceptin neurons. They also imply that the nociceptin system may modulate a variety of neurons in central nervous system sites, including the sensory and auditory pathways and centers implicated in emotion and autonomic control.

Hearing ability in mice lacking the nociceptin receptor

With the evidence for nociceptin and its receptor in brainstem auditory stations as shown above, we then examined the hearing ability of the mutant mice. Morphologically, the middle and inner ears and acoustic nerve of the mutant mice appeared normal (data not shown). The auditory brainstem responses (ABRs) measured in untreated mutant mice showed normal waveforms and thresholds (average threshold value: 37 dB SPL), which are comparable with those obtained in control mice (Colvin *et al.*, 1996). However, following exposure to intense sound, the thresholds of ABRs in the homozygous mutants showed a significant rise (Figure 6A). The threshold shift was considered temporary because the ABRs recovered completely to normal levels within 3 days (Figure 6B). Neither C57BL nor 129 strain mice showed the threshold shift. It is unlikely, therefore, that the shift is due to the heterogeneity in the genetic background. The results indicate that the nociceptin system is essential for the regulation of hearing ability following exposure to sound.

The mechanism of the disregulation remains to be investigated. We have shown abundant nociceptin precursor messages in the periolivary region (Figure 5), which is the principal site of the origin of efferent fibers, termed the crossed olivocochlear bundle, to the cochlear hair cells (Vetter *et al.*, 1991; Brown, 1993; Simmons *et al.*, 1996). Unlike other sensory systems, these efferent neurons present outstanding features for the auditory system because they have pivotal roles in directly influencing both the central auditory nuclei and the periphery (Brown, 1993). Stimulation or surgical impairment of the olivocochlear bundle has been shown to produce changes in cochlear mechanics, afferent fiber activities and efficiencies of signal detection (Dewson, 1968; Borg, 1971; Klinke and Galley, 1974; Mountain, 1980; Cody and Johnstone, 1982). The nociceptin system may modulate the excitability of the olivocochlear bundle and/or cochlear

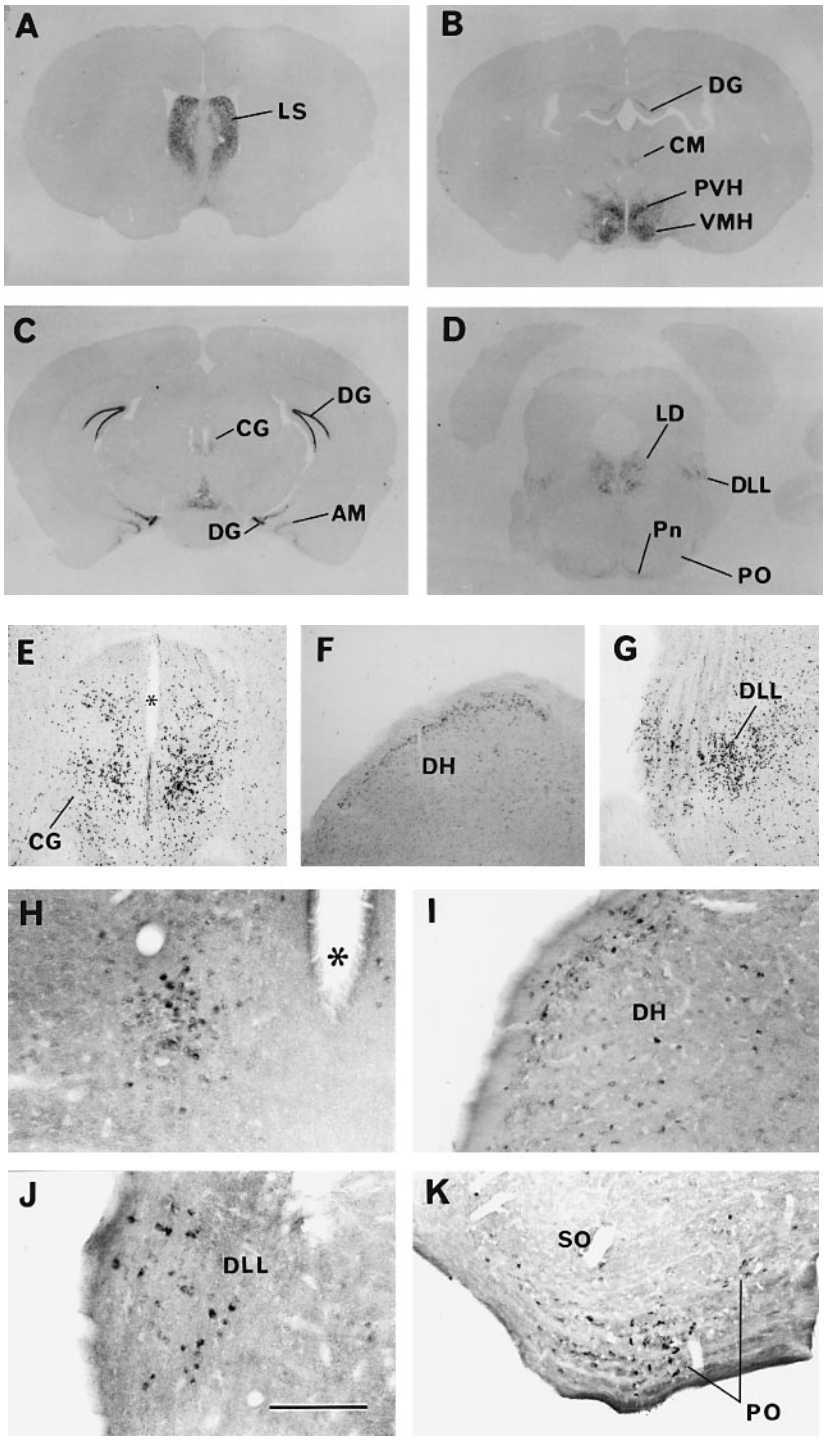

Fig. 5. (**A**–**G**) Expression of β-galactosidase activity in the brain and spinal cord in the nociceptin receptor-deficient mouse. β-Galactosidase activity is seen at high levels in the lateral septum (LS), granule cells of the dentate gyrus (DG), paraventricular hypothalamic nucleus (PVH), ventromedial hypothalamic nucleus (VMH), laterodorsal tegmental nucleus (LD) and dorsal division of the nucleus of the lateral lemniscus (DLL); it is also seen at moderate levels in the central medial thalamic nucleus (CM), corticomedial amygdaloid nucleus (AM), central gray (CG), pontine nuclei (Pn), periolivary region (PO) surrounding the superior olive and superficial layers (laminae I and II) of the dorsal horn (DH) in the spinal cord. The heterozygous mice displayed a similar pattern of β-galactosidase activity, but wild-type mice failed to show any enzyme activity. (**H**–**K**) Distribution of cells expressing nociceptin precursor mRNA in distinct sites of the sensory and auditory pathways. Representative are the CG and superficial DH layers of the spinal cord, the sites involved in sensory modulation (CG) and gate control of peripheral inputs (DH), and the DLL and PO, the sites involved in brainstem auditory relay (DLL) and centrifugal control of the cochlear outer hair cells (PO). Asterisks (E and H) indicate cerebral aqueduct. SO, superior olive. A sense probe failed to yield any hybridization signal (not shown). Scale bar, 2.3 mm (A–D), 500 μm (E–G), 200 μm (H–K).

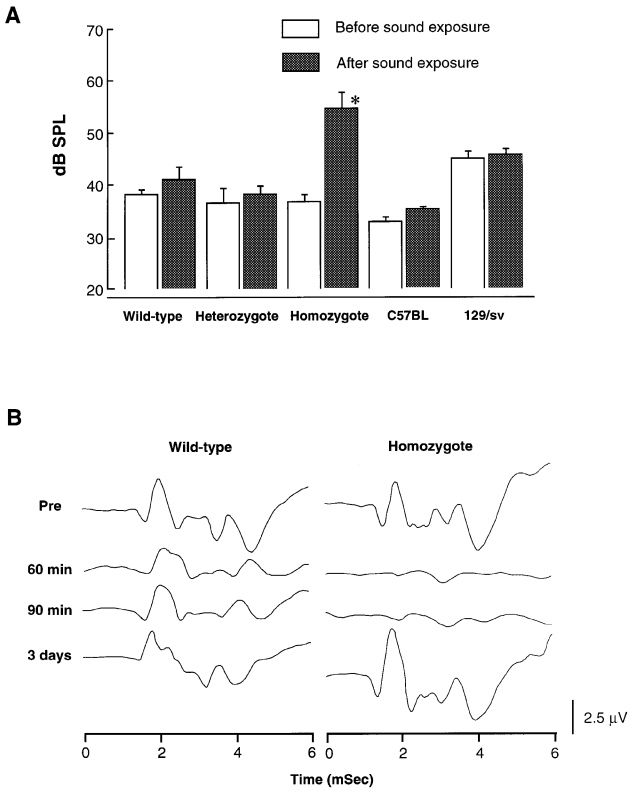

Fig. 6. Sound-induced threshold shifts of auditory brainstem responses (ABRs) in nociceptin receptor-deficient mice. (**A**) Thresholds of ABRs measured before and 60 min after sound exposure (110 dB). After sound exposure, the homozygous mutants displayed a significant rise in ABR thresholds. In contrast, all the other mice showed no distinct changes. Thresholds of ABRs were the lowest intensities (dB SPL) of click sound below which significant ABR waves disappeared, and are presented as means ± SEM ($n = 7$ in each group). The data were analyzed by ANOVA followed by a post-hoc Fisher's PLSD; the comparisons of threshold values between pre- and post-sound exposure are significant only in the homozygous mutants ($*P < 0.01$). (**B**) Temporal profiles of ABRs at 50 dB SPL from a wild-type mouse and a nociceptin receptor-deficient mutant. Both mice showed normal ABR patterns at pre-sound exposure and 3 days after sound exposure; however, the waveforms diminished to no response at 60 and 90 min only in the mutant mouse.

hair cells for the regulation of the auditory system. The present results provide a model system suitable for the investigation of the molecular mechanism of hearing ability and sound injury.

Materials and methods

Generation of mutant mice

The targeting vector was constructed using the genomic DNA fragments derived from λMORG5 (Nishi *et al.*, 1994), a synthetic polylinker carrying *Sac*I, *Xba*I and *Hin*dIII sites, the 3.7 kb *Hin*dIII–*Bam*HI fragment from pCH110 (Pharmacia Biotec.), the 1.1 kb *Xho*I–*Bam*HI fragment from pMC1 Neo poly(A) (Stratagene) and the ~3 kb *Xho*I–*Sal*I fragment containing the virus thymidine kinase gene (Takeshima *et al.*, 1994) and pBluescript SK(–) (Stratagene). The short arm of the vector is the 2.0 kb *Spe*I–*Rsa*I fragment containing the putative promoter and 5′-untranslated sequences, and the long arm is the 8.5 kb *Spe*I–*Sal*I (vector) fragment containing the second and third protein-coding sequences. The vector was linearized with *Not*I and transfected into J1 ES cells (Li *et al.*, 1992). Of ~250 clones screened by Southern blotting, we identified four clones carrying the homologous mutation. Chimeric mice produced with two clones (numbered 301 and 378) of the positive ES clones could transmit the mutation to their pups. Young adult mice (9–12 weeks old) were used for the analyses in this report. Blot hybridization analyses of DNA and RNA preparations from tissues of adult mice were performed as described previously (Takeshima *et al.*, 1994).

Behavioral analyses

Male mice were used for behavioral analyses. Analgesia was determined using the radiant heat, tail-flick technique (D'Amour and Smith, 1941). The latency to withdraw the tail from a focused light stimulus was measured electronically, using a photocell. For analyzing the effects of nociceptin, the latencies were measured 10 min after administration of nociceptin (1 or 10 nmol, i.c.v.) and were compared with baseline latencies. To examine the effects of morphine (10 mg/kg, s.c.) the latencies in mice were determined 60 min after administration. We used a higher intensity of light stimulation to examine the morphine-induced anti-nociceptive effects and a lower intensity to analyze the nociceptin-induced hyperalgesic effects. The maximum latency to response of 15 and 20 s would not induce tissue damage in mice treated with morphine and nociceptin, respectively.

Mice tested in the writhing assay received an injection (10 ml/kg, i.p.) of 0.7% acetic acid. The number of writhes, characterized by a wave of contraction of the abdominal muscles followed by extension of the hind limbs, was counted for 10 min, beginning 5 min after the injection.

To determine locomotor activity (Noda *et al.*, 1995), each animal was placed individually in a transparent acrylic cage (26×44×40 cm) and the locomotor count was recorded over 30 min using digital counters with infrared cell sensors placed on the walls (SCANET SV-10, Toyo-sangyo Co., Japan). To examine the effects of nociceptin, mice were injected with nociceptin (1 or 10 nmol, i.c.v.) and 10 min later the locomotor activities of the mice were measured. Experiments were carried out from 11:00 to 15:00.

Anatomical analyses

For β-galactosidase staining, mice were perfused with a 2% paraformaldehyde solution buffered with 0.12 M sodium phosphate (pH 7.4) under pentobarbital anesthesia, and the brains and spinal cords were immersed immediately in ice-cold 25% sucrose. Frozen coronal sections (40 μm thickness) were stained with the X-Gal reagent (Bajocchi *et al.*, 1993). For *in situ* hybridization, mice were perfused with a fixative containing 4% paraformaldehyde, 2% glutaraldehyde and 0.12 M sodium phosphate (pH 7.4). Brains and spinal cords were cut into coronal sections (50 μm thickness) and analyzed with the probe for nociceptin precursor mRNA as described previously (Houtani *et al.*, 1996).

Auditory brainstem responses

ABRs were measured (Colvin *et al.*, 1996) before and after sound exposure using chloral hydrate-administered mice by means of stepwise 0.1 ms click sound stimulations. Intense sound (1 kHz continuous pure tone at 110 dB SPL for 60 min) was applied to the mice in a soundproof room.

Acknowledgements

We thank Misa Shimuta, Ichiro Saito, Yoshinobu Sugitani and Hitomi Yamanaka for help in some experiments. This work was supported in part by Grants from the Ministry of Education, Science, Sports and Culture, the Japan Private School Promotion Foundation, the Naito Foundation, the Uehara Memorial Foundation, the Japanese Foundation of Metabolism and Diseases, the Ichiro Kanehara Foundation and the Mitsubishi Foundation.

References

Bajocchi,G., Feldman,S.H., Crystal,R.G. and Mastrangeli,A. (1993) Direct *in vivo* gene transfer to ependymal cells in the central nervous system using recombinant adenovirus vectors. *Nature Genet.*, **3**, 229–234.

Borg,E. (1971) Efferent inhibition of afferent acoustic activity in the unanesthetized rabbit. *Exp. Neurol.*, **31**, 301–312.

Brown,M.C. (1993) Fiber pathways and branching patterns of biocytin-labeled olivocochlear neurons in the mouse brainstem. *J. Comp. Neurol.*, **337**, 600–613.

Bunzow,J.R., Saez,C., Mortrud,M., Bouvier,C., Williams,J.T., Low,M. and Grandy,D.K. (1994) Molecular cloning and tissue distribution of a putative member of the rat opioid receptor gene family that is not a μ, δ or κ opioid receptor type. *FEBS Lett.*, **347**, 284–288.

Cody,A.R. and Johnstone,B.M. (1982) Temporary threshold shift modified by binaural acoustic stimulation. *Hearing Res.*, **6**, 199–205.

Colvin,J.S., Bohne,B.A., Harding,G.W., McEwen,D.G. and Ornitz,D.M. (1996) Skeletal overgrowth and deafness in mice lacking fibroblast growth factor receptor 3. *Nature Genet.*, **12**, 390–397.

D'Amour,F.E. and Smith,D.L. (1941) A method for determining loss of pain sensation. *J. Pharmacol. Exp. Ther.*, **72**, 74–79.

Dewson,J.H.,III (1968) Efferent olivocochlear bundle: some relationships to stimulus discrimination in noise. *J. Neurophysiol.*, **31**, 122–130.

Fukuda,K., Kato,S., Mori,K., Nishi,M., Takeshima,H., Iwabe,N., Miyata,T., Houtani,T. and Sugimoto,T. (1994) cDNA cloning and regional distribution of a novel member of the opioid receptor family. *FEBS Lett.*, **343**, 42–46.

Gerlai,R. (1996) Gene-targeting studies of mammalian behavior: is it the mutation or the background genotype? *Trends Neurosci.*, **19**, 177–181.

Halford,W.P., Gebhardt,B.M. and Carr,D.J.J. (1995) Functional role and sequence analysis of a lymphocyte orphan opioid receptor. *J. Neuroimmunol.*, **59**, 91–101.

Hille,B. (1992) G protein-coupled mechanisms and nervous signaling. *Neuron*, **9**, 187–195.

Houtani,T., Nishi,M., Takeshima,H., Nukada,T. and Sugimoto,T. (1996) Structure and regional distribution of nociceptin/orphanin FQ precursor. *Biochem. Biophys. Res. Commun.*, **219**, 714–719.

Klinke,R. and Galley,N. (1974) Efferent innervation of vestibular and auditory receptors. *Physiol. Rev.*, **54**, 316–357.

Knapp,R.J., Malatynska,E., Collins,N., Fang,L., Wang,J.Y., Hruby,V.J., Roeske,W.R. and Yamamura,H.I. (1995) Molecular biology and pharmacology of cloned opioid receptors. *FASEB J.*, **9**, 516–525.

Li,E., Bestor,T.H. and Jaenisch,R. (1992) Targeted mutation of the DNA methyltransferase gene results in embryonic lethality. *Cell*, **69**, 915–926.

Loh,H.H. and Smith,A.P. (1990) Molecular characterization of opioid receptors. *Annu. Rev. Pharmacol. Toxicol.*, **30**, 123–147.

Matthes,H.W.D. *et al*. (1996) Loss of morphine-induced analgesia, reward effect and withdrawal symptoms in mice lacking the μ-opioid-receptor gene. *Nature*, **383**, 819–823.

Meunier,J.-C. *et al*. (1995) Isolation and structure of the endogenous agonist of opioid receptor-like ORL1 receptor. *Nature*, **377**, 532–535.

Mollereau,C., Parmentier,M., Mailleux,P., Butour,J.-L., Moisand,C., Chalon,P., Caput,D., Vassart,G. and Meunier,J.-C. (1994) ORL1, a novel member of the opioid receptor family. Cloning, functional expression and localization. *FEBS Lett.*, **341**, 33–38.

Mollereau,C., Simons,M.-J., Soularue,P., Liners,F., Vassart,G., Meunier,J.-C. and Parmentier,M. (1996) Structure, tissue distribution, and chromosomal localization of the prepronociceptin gene. *Proc. Natl Acad. Sci. USA*, **93**, 8666–8670.

Mountain,D.C. (1980) Changes in endolymphatic potential and crossed olivocochlear bundle stimulation alter cochlear mechanics. *Science*, **210**, 71–72.

Nishi,M., Takeshima,H., Mori,M., Nakagawara,K. and Takeuchi,T. (1994) Structure and chromosomal mapping of genes for the mouse κ-opioid receptor and an opioid receptor homologue (MOR-C). *Biochem. Biophys. Res. Commun.*, **205**, 1353–1357.

Noda,Y., Yamada,K., Furukawa,H. and Nabeshima,T. (1995) Involvement of nitric oxide in phencyclidine-induced hyperlocomotion in mice. *Eur. J. Pharmacol.*, **286**, 291–297.

Nothacker,H.-P., Reinscheid,R.K., Mansour,A., Henningsen,R.A., Ardati,A., Monsma,F.J.,Jr, Watson,S.J. and Civelli,O. (1996) Primary structure and tissue distribution of the orphanin FQ precursor. *Proc. Natl Acad. Sci.USA*, **93**, 8677–8682.

Okuda-Ashitaka,E., Tachibana,S., Houtani,T., Minami,T., Masu,Y., Nishi,M., Takeshima,H., Sugimoto,T. and Ito,S. (1996) Identification and characterization of an endogenous ligand for opioid receptor homologue ROR-C: its involvement in allodynic response to innocuous stimulus. *Mol. Brain Res.*, **43**, 96–104.

Reinscheid,R.K. *et al*. (1995) Orphanin FQ: a neuropeptide that activates an opioidlike G protein-coupled receptor. *Science*, **270**, 792–794.

Saito,Y., Maruyama,K., Kawano,H., Hagino-Yamagishi,K., Kawamura,K., Saido,T.C. and Kawashima,S. (1996) Molecular cloning and characterization of a novel form of neuropeptide gene as a developmentally regulated molecule. *J. Biol. Chem.*, **271**, 15615–15622.

Simmons,D.D., Mansdorf,N.B. and Kim,J.H. (1996) Olivocochlear innervation of inner and outer hair cells during postnatal maturation: evidence for a waiting period. *J. Comp. Neurol.*, **370**, 551–562.

Takeshima,H., Iino,M., Takekura,H., Nishi,M., Kuno,J., Minowa,O., Takano,H. and Noda,T. (1994) Excitation–contraction uncoupling and muscular degeneration in mice lacking functional skeletal muscle ryanodine-receptor gene. *Nature*, **369**, 556–559.

Vetter,D.E., Adams,J.C. and Mugnaini,E. (1991) Chemically distinct rat olivocochlear neurons. *Synapse*, **7**, 21–43.

Wick,M.J., Minnerath,S.R., Roy,S., Ramakrishnan,S. and Loh,H.H. (1995) Expression of alternate forms of brain opioid 'orphan' receptor mRNA in activated human peripheral blood lymphocytes and lymphocytic cell lines. *Mol. Brain Res.*, **32**, 342–347.

Received on September 27, 1996; revised on November 26, 1996